Applied Mathematics and Computation 371 (2020) 124933

Contents lists available at ScienceDirect

Applied Mathematics and Computation

journal homepage: www.elsevier.com/locate/amc

Analytical and computational approaches on solitary wave solutions of the generalized equal width equation

Seydi Battal GaziKarakoc[a], Khalid K. Ali[b,*]

[a] Department of Mathematics, Faculty of Science and Art, Nevsehir Haci Bektas Veli University, Nevsehir 50300, Turkey
[b] Department of Mathematics, Faculty of Science, AL-Azhar University Nasr City, P.N. Box: Cairo 11884, Egypt

ARTICLE INFO

Article history:
Received 3 September 2018
Revised 4 August 2019
Accepted 24 November 2019
Available online 17 December 2019

MSC:
65N30
65D07
74S05
74J35
76B25

Keywords:
GEW equation
Petrov-Galerkin
The modified extended tanh method
Cubic B-splines
Solitary waves
Soliton

ABSTRACT

In this article, firstly numerical solutions of the generalized equal width (GEW) equation have been obtained by a Petrov-Galerkin finite element method using cubic B-spline base functions as element shape functions and quadratic B-spline base functions as the weight functions. In order to prove the practicability and robustness of the numerical algorithm, the error norms L_2, L_∞ and three invariants I_1, I_2 and I_3 are computed. A linear stability analysis based on a Fourier method states that the numerical scheme is unconditionally stable. Secondly, we have proposed the modified extended tanh-function method with the Riccati differential equation, which is a convenient and an effective method, for getting the exact traveling wave solutions of the equation. Motion of single solitary wave is examined using the present methods. The obtained results are indicated both in tabular and graphical form.

1. Introduction

Nonlinear wave phenomena appear in many fields, such as fluid mechanics, plasma physics, applied mathematics, in engineering problems, biology, hydrodynamics, solid state physics and optical fibers. In order to better understand these nonlinear phenomena, it is important to explore their exact solutions. The tanh-function method ensures an effective and direct algebraic method for solving nonlinear equations. Based on the localized nature of soliton solutions, the tanh-function method overcomes the complex integration process to get explicit solutions to various types of nonlinear equations. The standard tanh method is improved by Malfiet [1]. In recent years, there was interest in obtaining exact solutions of nonlinear partial differential equation (PDE) by the extended tanh method. Wazwaz examined exact solutions of nonlinear partial differential equation by the extended tanh method [2–4]. Fan and Hon [5] submitted a generalized tanh method for constructing the exact solutions of nonlinear partial differential equation, such as, the (2+1)-dimensional sine-Gordon equation and the double sine-Gordon equation. In particular, the modified extended tanh-function method [6,7] is widely identified as one of the most powerful tools used recently in a favor of searching for explicit solitary travelling wave solutions PDE's. But exact solutions of PDE's are commonly not derivable, particularly when the nonlinear terms are contained. In so far

* Corresponding author at: Department of Mathematics, Faculty of Science, AL-Azhar University Nasr City, P.N. Box: 11884 Cairo, Egypt.
E-mail addresses: sbgkarakoc@nevsehir.edu.tr (S.B. GaziKarakoc), khalidkaram2012@yahoo.com (K.K. Ali).

https://doi.org/10.1016/j.amc.2019.124933
0096-3003/

as only limited classes of these equations are solved by analytical means, numerical solutions of these nonlinear partial differential equations are very operable to examine physical phenomena. The regularized long wave (RLW) equation,

$$U_t + U_x + \varepsilon UU_x - \mu U_{xxt} = 0, \tag{1}$$

is modelled to manage a broad number of physical developments for instance the nonlinear transverse waves in shallow water, ion-acoustic waves in plasma, hydromagnetic wave in cold plasma, plasma, elastic media, optical fibres, acoustic-gravity waves in compressible fluids, pressure waves in liquid–gas bubbles and acoustic waves inharmonic crystals. It was first alleged as a model for small-amplitude long-waves on the surface of water in a channel by Peregrine [8,9]. Benjamin et al. [10] presented the RLW equation as a logical alternative model to the more common

$$U_t + U_x + aUU_x - bU_{xxt} = 0, \tag{2}$$

Korteweg-de Vries (KdV) equation. The KdV equation plays an important role in describing motions of long waves in shallow water under gravity, one-dimensional nonlinear lattice, fluid mechanics, quantum mechanics, plasma physics and nonlinear optics. Morrison et al. [11] have proposed an equally valid alternative, the following equal width (EW) equation

$$U_t + \varepsilon UU_x - \mu U_{xxt} = 0, \tag{3}$$

both as a model partial differential equation for the simulation of one-dimensional wave propagation in nonlinear media with dispersion processes and as an alternative model of nonlinear dispersive waves to the well known the RLW and KdV equations. The solutions of this equation are types of solitary waves called as solitons whose forms are not changed after the collision. The GEW equation considered here has the following normalized form

$$U_t + \varepsilon U^p U_x - \delta U_{xxt} = 0, \tag{4}$$

where p is a positive integer, ε and δ positive parameters, t is time and x is the space coordinate, $U(x, t)$ is the wave amplitude. Physical boundary conditions require $U \to 0$ as $|x| \to \infty$. For this study, boundary and initial conditions are taken

$$\begin{aligned} U(a,t) &= 0, & U(b,t) &= 0, \\ U_x(a,t) &= 0, & U_x(b,t) &= 0, \\ U_{xx}(a,t) &= 0, & U_{xx}(b,t) &= 0, \\ U(x,0) &= f(x), & a \le x \le b, \end{aligned} \tag{5}$$

where $f(x)$ is a localized disturbance inside the considered interval and will be determined later. In the fluid problems as known, the quantity U defines the wave amplitude of the water surface or a similar physical quantity. In the plasma implementations, U is the negative of the electrostatic potential. That's why, the solitary wave solution of Eq. (4) helps us to better understand the many physical phenomena with weak nonlinearity and dispersion waves such as nonlinear transverse waves in shallow water, ion-acoustic and magneto- hydrodynamic waves in plasma and phonon packets in nonlinear crystals [12]. The GEW equation which we tackle here is based on the EW equation and depend on the both generalized regularized long wave (GRLW) equation [13,14] and the generalized Korteweg-de Vries (GKdV) equation [15]. These general equations are nonlinear wave equations with $(p+1)$th nonlinearity and have solitary wave solutions, which are pulse-like.The study of GEW equation provides the opportunity of investigating the creation of secondary solitary waves and/or radiation to get insight into the corresponding processes of particle physics [16,17]. This equation has many applications in physical situations such as unidirectional waves propagating in a water channel, long waves in near-shore zones, and many others [18]. If we take $p = 1$ in Eq. (4) we get the EW equation and [19–25] and if we take $p = 2$, the obtained equation is called as the modified equal width wave (MEW) equation [26–32]. In the literature, there are limited number of papers on the GEW equation. Hamdi et al. [33] derived exact solitary wave solutions of the GEW equation. Evans and Raslan [34] considered the GEW equation by using the collocation method based on quadratic B-splines to obtain the numerical solutions of the single solitary wave, interaction of solitary waves and birth of solitons. The GEW equation solved numerically by a cubic B-spline collocation method by Raslan [19]. The homogeneous balance method was used to construct exact travelling wave solutions of generalized equal width equation by Taghizadeh et al. [35]. The generalized equal width (GEW) equation was solved numerically by a meshless method based on a global collocation with standard types of radial basis functions (RBFs) by [18]. Quintic B-spline collocation method with two different linearization techniques and a lumped Galerkin method based on cubic B-spline functions were employed to obtain the numerical solutions of the GEW equation by Karakoc and Zeybek, [12,36] respectively. Roshan [37], implemented Petrov-Galerkin method using the linear hat function and quadratic B-spline function as test and trial functions respectively for the GEW equation.

In this study, we have designed a lumped Petrov-Galerkin method and the modified extended tanh function method with Riccati equation for the GEW equation. The plan of this paper is as follows: In Section 2, a lumped Petrov-Galerkin finite element technique has been practiced to GEW equation. Resulting system can be solved with a sort of the Thomas algorithm. A linear stability analysis of the scheme is examined in Section 3. In Section 4, motion of single solitary wave has been analyzed for the problem with different initial and boundary conditions. The acquired numerical results are given both in tabular and graphical form and the computed results are also hold a candle to some of those available in the literature. In Section 5, description of the modified extended tanh function method with the Riccati equation is presented. In Section 6, we apply the proposed modified extended tanh function method to get the exact solutions for GEW equation. Conclusions are given in Section 7.

2. Analysis of the Petrov-Galerkin method

Let us consider the solution domain is limited to a finite interval $a \le x \le b$. Partition the interval $[a, b]$ at points by x_m where $a = x_0 < x_1 < \ldots < x_N = b$ and let $h = \frac{b-a}{N}$, $m = 0, 1, 2, \ldots, N$. On this partition, we shall need the following cubic B-splines $\phi_m(x)$ at the points x_m, $m = 0, 1, 2, \ldots, N$. Prenter [38] defined following cubic B-spline functions $\phi_m(x)$, ($m = -1(1) N+1$), at the points x_m which compose a basis over the region $[a, b]$ by

$$\phi_m(x) = \frac{1}{h^3}\begin{cases} (x - x_{m-2})^3, & x \in [x_{m-2}, x_{m-1}), \\ h^3 + 3h^2(x - x_{m-1}) + 3h(x - x_{m-1})^2 - 3(x - x_{m-1})^3, & x \in [x_{m-1}, x_m), \\ h^3 + 3h^2(x_{m+1} - x) + 3h(x_{m+1} - x)^2 - 3(x_{m+1} - x)^3, & x \in [x_m, x_{m+1}), \\ (x_{m+2} - x)^3, & x \in [x_{m+1}, x_{m+2}], \\ 0 & otherwise. \end{cases} \tag{6}$$

A global approximation $U_N(x, t)$ is stated in terms of cubic B-splines by

$$U_N(x, t) = \sum_{j=-1}^{N+1} \phi_j(x)\delta_j(t), \tag{7}$$

in which parameters $\delta_j(t)$ are obtained using boundary and weighted residual conditions. A typical finite interval $[x_m, x_{m+1}]$ is converted to more easily operable interval [0,1] with a local coordinate transformation defined by $h\eta = x - x_m$ ($0 \le \eta \le 1$). Thus cubic B-splines (6) depending on variable η can be given as follows:

$$\begin{aligned} \phi_{m-1} &= (1 - \eta)^3, \\ \phi_m &= 1 + 3(1 - \eta) + 3(1 - \eta)^2 - 3(1 - \eta)^3, \\ \phi_{m+1} &= 1 + 3\eta + 3\eta^2 - 3\eta^3, \\ \phi_{m+2} &= \eta^3. \end{aligned} \tag{8}$$

Cubic B-splines except $\phi_{m-1}(x), \phi_m(x), \phi_{m+1}(x), \phi_{m+2}(x)$ and their four principal derivatives vanish the outside of the region [0,1]. Hence approximation function (7) in terms of element parameters $\delta_{m-1}, \delta_m, \delta_{m+1}, \delta_{m+2}$ and B-spline element functions $\phi_{m-1}, \phi_m, \phi_{m+1}, \phi_{m+2}$ are given over the region [0,1] by

$$U_N(\eta, t) = \sum_{j=m-1}^{m+2} \delta_j\phi_j. \tag{9}$$

Using equalities (8) and (9), approximation of nodal values U_m and its first and second derivatives are obtained as follows:

$$\begin{aligned} U_m &= U(x_m) = \delta_{m-1} + 4\delta_m + \delta_{m+1}, \\ U'_m &= U'(x_m) = 3(-\delta_{m-1} + \delta_{m+1}), \\ U''_m &= U''(x_m) = 6(\delta_{m-1} - 2\delta_m + \delta_{m+1}). \end{aligned} \tag{10}$$

We take the weight functions Φ_m as quadratic B-splines. The quadratic B-splines Φ_m at the knots x_m are defined as [38]:

$$\Phi_m(x) = \frac{1}{h^2}\begin{cases} (x_{m+2} - x)^2 - 3(x_{m+1} - x)^2 + 3(x_m - x)^2, & x \in [x_{m-1}, x_m), \\ (x_{m+2} - x)^2 - 3(x_{m+1} - x)^2, & x \in [x_m, x_{m+1}), \\ (x_{m+2} - x)^2, & x \in [x_{m+1}, x_{m+2}), \\ 0 & otherwise. \end{cases} \tag{11}$$

Using the local coordinate transformation for the finite element $[x_m, x_{m+1}]$ by $h\eta = x - x_m$ ($0 \le \eta \le 1$) quadratic B-splines Φ_m are given as

$$\begin{aligned} \Phi_{m-1} &= (1 - \eta)^2, \\ \Phi_m &= 1 + 2\eta - 2\eta^2, \\ \Phi_{m+1} &= \eta^2. \end{aligned} \tag{12}$$

Performing the Petrov-Galerkin method to Eq. (4), the weak form of Eq. (4) is attained as

$$\int_a^b \Phi(U_t + \varepsilon U^p U_x - \mu U_{xxt})dx = 0. \tag{13}$$

For a unique element $[x_m, x_{m+1}]$ using transformation $h\eta = x - x_m (0 \le \eta \le 1)$ into Eq. (13), we obtain the following integral equation:

$$\int_0^1 \Phi\left(U_t + \frac{\varepsilon}{h}\hat{U}^p U_\eta - \frac{\mu}{h^2}U_{\eta\eta t}\right)d\eta = 0, \tag{14}$$

where $\hat{U}$ is approved to be constant over an element to facilitate the integral. Integrating Eq. (14) by parts and using Eq. (4) which yields:

$$\int_0^1 [\Phi(U_t + \lambda U_\eta) + \beta \Phi_\eta U_{\eta t}]d\eta = \beta \Phi U_{\eta t}|_0^1, \tag{15}$$

where $\lambda = \frac{\varepsilon \hat{U}^p}{h}$ and $\beta = \frac{\mu}{h^2}$. Assuming the weight function Φ_i with quadratic B-spline shape functions given by Eq. (11) and substituting approximation (9) into integral Eq. (15), we get the element contributions in the form:

$$\sum_{j=m-1}^{m+2} \left[\left(\int_0^1 \Phi_i \phi_j + \beta \Phi_i' \phi_j' \right) d\eta - \beta \Phi_i \phi_j' |_0^1 \right] \dot{\delta}_j^e + \sum_{j=m-1}^{m+2} \left(\lambda \int_0^1 \Phi_i \phi_j' d\eta \right) \delta_j^e = 0, \tag{16}$$

where $\delta^e = (\delta_{m-1}, \delta_m, \delta_{m+1}, \delta_{m+2})^T$ are the element parameters and dot states differentiation to t which can be written in matrix form as follows:

$$[A^e + \beta(B^e - C^e)]\dot{\delta}^e + \lambda D^e \delta^e = 0. \tag{17}$$

The element matrices $A_{ij}^e, B_{ij}^e, C_{ij}^e$ and D_{ij}^e are rectangular 3×4 given by the following integrals;

$$A_{ij}^e = \int_0^1 \Phi_i \phi_j d\eta = \frac{1}{60} \begin{bmatrix} 10 & 71 & 38 & 1 \\ 19 & 221 & 221 & 19 \\ 1 & 38 & 71 & 10 \end{bmatrix},$$

$$B_{ij}^e = \int_0^1 \Phi_i' \phi_j' d\eta = \frac{1}{2} \begin{bmatrix} 3 & 5 & -7 & -1 \\ -2 & 2 & 2 & -2 \\ -1 & -7 & 5 & 3 \end{bmatrix},$$

$$C_{ij}^e = \Phi_i \phi_j' |_0^1 = 3 \begin{bmatrix} 1 & 0 & -1 & 0 \\ 1 & -1 & -1 & 1 \\ 0 & -1 & 0 & 1 \end{bmatrix},$$

$$D_{ij}^e = \int_0^1 \Phi_i \phi_j' d\eta = \frac{1}{10} \begin{bmatrix} -6 & -7 & 12 & 1 \\ -13 & -41 & 41 & 13 \\ -1 & -12 & 7 & 6 \end{bmatrix},$$

where i takes the values $m-1, m, m+1$ and the j takes the values $m-1, m, m+1, m+2$ for the typical element $[x_m, x_{m+1}]$. A lumped value for U is got from $(\frac{U_m + U_{m+1}}{2}^p)$ as

$$\lambda = \frac{\varepsilon}{2^p h} (\delta_{m-1} + 5\delta_m + 5\delta_{m+1} + \delta_{m+2})^p.$$

Assembling all contributions coming from all the elements, matrix Eq. (17) yields the following system

$$[A + \beta(B - C)]\dot{\delta} + \lambda D \delta = 0, \tag{18}$$

where $\delta = (\delta_{-1}, \delta_0, \ldots, \delta_N, \delta_{N+1})^T$ are global element parameters. *A, B, C* and λD are global matrices and each generalized mth row of the global matrices is as follows:

$$A = \frac{1}{60}(1, 57, 302, 302, 57, 1, 0), B = \frac{1}{2}(-1, -9, 10, 10, -9, -1, 0),$$
$$C = (0, 0, 0, 0, 0, 0, 0)$$
$$\lambda D = \frac{1}{10} \begin{pmatrix} -\lambda_1, -12\lambda_1 - 13\lambda_2, 7\lambda_1 - 41\lambda_2 - 6\lambda_3, 6\lambda_1 + 41\lambda_2 - 7\lambda_3, \\ 13\lambda_2 + 12\lambda_3, \lambda_3, 0 \end{pmatrix}$$

where

$$\lambda_1 = \frac{\varepsilon}{2^p h} (\delta_{m-2} + 5\delta_{m-1} + 5\delta_m + \delta_{m+1})^p, \ \lambda_2 = \frac{\varepsilon}{2^p h} (\delta_{m-1} + 5\delta_m + 5\delta_{m+1} + \delta_{m+2})^p,$$
$$\lambda_3 = \frac{\varepsilon}{2^p h} (\delta_m + 5\delta_{m+1} + 5\delta_{m+2} + \delta_{m+3})^p.$$

Replacing the time derivative $\dot{\delta}$ by the forward difference approximation $\dot{\delta} = \frac{\delta^{n+1} - \delta^n}{\Delta t}$ and the parameter δ by the Crank-Nicolson formulation $\delta = \frac{1}{2}(\delta^n + \delta^{n+1})$, then Eq. (17) reduce to the following matrix system:

$$\left[A + \beta(B - C) + \frac{\lambda \Delta t}{2} D \right] \delta^{n+1} = \left[A + \beta(B - C) - \frac{\lambda \Delta t}{2} D \right] \delta^n, \tag{19}$$

where t is time step. Practicing the boundary conditions (5) to the (19), $(N+1)\times(N+1)$ matrix system is obtained. This result system is efficiently solved with a variant of the Thomas algorithm but in solution process, two or three inner iterations $\delta^{n*}=\delta^{n}+\frac{1}{2}(\delta^{n}-\delta^{n-1})$ are also implemented at each time step to improve the accuracy. Consequently, a typical member of the matrix system (19) may be written in terms of the nodal parameters system repetition connection between time steps δ^{n} and δ^{n+1} as:

$$\begin{aligned}&\gamma_1\delta_{m-2}^{n+1}+\gamma_2\delta_{m-1}^{n+1}+\gamma_3\delta_{m}^{n+1}+\gamma_4\delta_{m+1}^{n+1}+\gamma_5\delta_{m+2}^{n+1}+\gamma_6\delta_{m+3}^{n+1}\\&\quad=\gamma_6\delta_{m-2}^{n}+\gamma_5\delta_{m-1}^{n}+\gamma_4\delta_{m}^{n}+\gamma_3\delta_{m+1}^{n}+\gamma_2\delta_{m+2}^{n}+\gamma_1\delta_{m+3}^{n},\end{aligned}\tag{20}$$

where

$$\gamma_1=\frac{1}{60}-\frac{\beta}{2}-\frac{\lambda\Delta t}{20},\qquad \gamma_2=\frac{57}{60}-\frac{9\beta}{2}-\frac{25\lambda\Delta t}{20},\quad \gamma_3=\frac{302}{60}+\frac{10\beta}{2}-\frac{40\lambda\Delta t}{20},$$
$$\gamma_4=\frac{302}{60}+\frac{10\beta}{2}+\frac{40\lambda\Delta t}{20},\quad \gamma_5=\frac{57}{60}-\frac{9\beta}{2}+\frac{25\lambda\Delta t}{20},\quad \gamma_6=\frac{1}{60}-\frac{\beta}{2}+\frac{\lambda\Delta t}{20}.$$

To begin the iteration, the initial vector δ^{0} is calculated by using the initial and boundary conditions. So, using the relations at the knots $U_N(x_m,0)=U(x_m,0),\ m=0,1,2,\ldots,N$ and $U_N'(x_0,0)=U'(x_N,0)=0$ associated with a variant of the Thomas algorithm, the initial vector δ^{0} is easily found from the following matrix form

$$\begin{bmatrix}-3&0&3&&&&\\1&4&1&&&&\\&&\ddots&&&&\\&&&1&4&1\\&&&-3&0&3\end{bmatrix}\begin{bmatrix}\delta_{-1}^{0}\\\delta_{0}^{0}\\\vdots\\\delta_{N}^{0}\\\delta_{N+1}^{0}\end{bmatrix}=\begin{bmatrix}U'(x_0,0)\\U(x_0,0)\\\vdots\\U(x_N,0)\\U'(x_N,0)\end{bmatrix}.$$

3. Stability analysis of the numerical method

Stability of the presented technique is explored by practicing Fourier method based on Von-Neumann theory. Presuming $U^{p}=\lambda$ in the nonlinear term $U^{p}U_x$ of GEW Eq. (4) is locally constant. Substituting the Fourier mode $\delta_j^{n}=g^{n}e^{ijkh}$ $(i=\sqrt{-1})$ where k is mode number and h is element greatness, into scheme (20), which generates the growth factor

$$g=\frac{a-ib}{a+ib},\tag{21}$$

where

$$\begin{aligned}a&=(302+300\beta)\cos\left(\frac{\theta}{2}\right)h+(57-270\beta)\cos\left(\frac{3\theta}{2}\right)h+(1-30\beta)\cos\left(\frac{5\theta}{2}\right)h,\\b&=120\lambda\Delta t\sin\left(\frac{\theta}{2}\right)h+75\lambda\Delta t\sin\left(\frac{3\theta}{2}\right)h+3\lambda\Delta t\sin\left(\frac{5\theta}{2}\right)h.\end{aligned}\tag{22}$$

The modulus of $|g|$ is 1, so the linearized scheme is unconditionally stable.

4. Numerical results and discussion

In this part, in order to verify of our numerical algorithm, we take into consideration some experiments involving: Dispersion of single solitary waves, interaction of two solitary waves and the Maxwellian initial condition are investigated. For these three problems, to demonstrate how suitable our numerical algorithm foresees the position and amplitude of the solution as the simulation progresses, we handle the following error norms:

$$L_2=\left\|U^{exact}-U_N\right\|_2\simeq\sqrt{h\sum_{J=0}^{N}\left|U_j^{exact}-(U_N)_j\right|^2},$$

and

$$L_\infty=\left\|U^{exact}-U_N\right\|_\infty\simeq\max_j\left|U_j^{exact}-(U_N)_j\right|.$$

The exact solution of the GEW equation is found to be [34,36]

$$U(x,t)=\sqrt[p]{\frac{c(p+1)(p+2)}{2\varepsilon}\sec h^2\left[\frac{p}{2\sqrt{\mu}}(x-ct-x_0)\right]}$$

Table 1
Invariants and errors for single solitary wave with $p = 2,\ c = 0.5, h = 0.1,\ \varepsilon = 3,\ \Delta t = 0.2,\ \mu = 1,\ x \in [0, 80]$.

Time	I_1	I_2	I_3	L_2	L_∞
0	3.1415863	2.6666583	1.3333283	0.00000000	0.00000000
5	3.1415911	2.6666744	1.3333406	0.00395938	0.00295270
10	3.1415916	2.6666753	1.3333413	0.00705757	0.00474584
15	3.1415916	2.6666753	1.3333413	0.00997382	0.00652868
20	3.1415916	2.6666753	1.3333413	0.01288981	0.00832796

Table 2
Comparisons of results for single solitary wave with $p = 2,\ c = 0.5, h = 0.1,\ \varepsilon = 3,\ \Delta t = 0.2,\ \mu = 1,\ x \in [0, 80]$ at $t = 20$.

Method	I_1	I_2	I_3	L_2	L_∞
Analytic	3.1415927	2.6666667	1.3333333	0.00000000	0.00000000
Our Method	3.1415916	2.6666753	1.3333413	0.01288981	0.00832796
Cubic Galerkin [12]	3.1589605	2.6902580	1.3570299	0.03803037	0.02629007
Quintic Collocation First Scheme [36]	3.1250343	2.6445829	1.3113394	0.05132106	0.03416753
Quintic Collocation Second Scheme [36]	3.1416722	2.6669051	1.3335718	0.01675092	0.01026391
Petrov-Galerkin [37]	3.14159	2.66673	1.33341	0.0123326	0.0086082

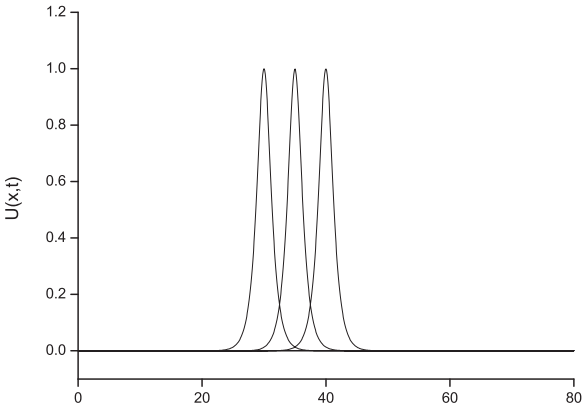

Fig. 1. Motion of single solitary wave for $p = 2,\ c = 0.5,\ h = 0.1,\ \Delta t = 0.2,\ \varepsilon = 3,\ \mu = 1$, over the interval [0, 80] at $t = 0, 10, 20$.

where c is the speed of the wave traveling in the positive direction of the x-axis and x_0 is arbitrary constant. There are three conserved quantities for the GEW equation. These are correspond to mass, momentum and energy given by

$$I_1 = \int_a^b U(x,t)dx, \qquad I_2 = \int_a^b [U^2(x,t) + \mu U_x^2(x,t)]dx, \qquad I_3 = \int_a^b U^{p+2}(x,t)dx \tag{23}$$

respectively.

4.1. Dispersion of a single solitary wave

For the first set, we choose the parameters $p = 2,\ c = 0.5,\ h = 0.1,\ \Delta t = 0.2,\ \mu = 1,\ \varepsilon = 3,\ x_0 = 30$ with interval [0,80] to match up with that of previous papers [12,36,37]. Hence the solitary wave has amplitude 1.0 and the program is run up to time $t = 20$ over the solution domain. Analytical values of the invariants are $I_1 = 3.1415927,\ I_2 = 2.6666667$ and $I_3 = 1.3333333$. Values of the three invariants as well as L_2 and L_∞-error norms from our method have been computed and listed in Table 1. Referring to Table 1, the error norms L_2 and L_∞ remain less than 1.288981×10^{-2} and 8.32796×10^{-3}, the invariants I_1, I_2 and I_3 change from their initial values by less than 5.3×10^{-6}, 1.7×10^{-5} and 1.3×10^{-5}, respectively, throughout the simulation. Also, our invariants are almost constant as time increases and the changes of the invariants agree with their exact values. So we can say our method is sensibly conservative. Comparisons with our results with exact solution as well as the recorded values in [12,36,37] have been made and tabulated in Table 2 at $t = 20$. This table clearly shows that the error norms got by our method are marginally less than the others. The motion of solitary wave using our scheme is plotted at time $t = 0, 10, 20$ in Fig. 1. As seen, single solitons move to the right at a constant speed and preserves its amplitude and shape with increasing time as anticipated. Initially, the amplitude of solitary wave is 1.00000 and its top position is pinpionted at $x = 30$. At $t = 20$, its amplitude is noted as 0.999416 with center $x = 40$. Thereby the absolute difference in amplitudes over the time interval [0,20] are observed as 5.84×10^{-4}. The quantile of error at discount times are depicted in Fig. 2. The error aberration varies from -8×10^{-2} to 1×10^{-2}.

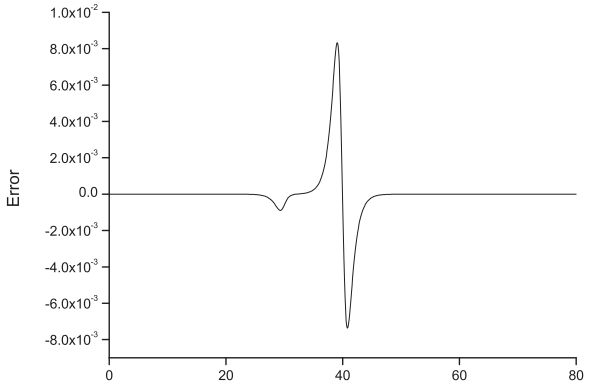

Fig. 2. Error graph for $p = 2,\ c = 0.5,\ h = 0.1,\ \varepsilon = 3,\ \Delta t = 0.2,\ \mu = 1,\ x \in [0, 80]$ at $t = 20$.

Table 3
Invariants and errors for single solitary wave with $p = 3,\ c = 0.3, h = 0.1,\ \Delta t = 0.2,\ \varepsilon = 3,\ \mu = 1,\ x \in [0, 80]$.

Time	I_1	I_2	I_3	L_2	L_∞
0	2.8043580	2.4639009	0.9855618	0.000000	0.000000
5	2.8043722	2.4639383	0.9855940	0.00184591	0.00179091
10	2.8043742	2.4639418	0.9855971	0.00294802	0.00235427
15	2.8043743	2.4639419	0.9855971	0.00376675	0.00288459
20	2.8043743	2.4639418	0.9855971	0.00454007	0.00341543

Table 4
Comparisons of results for single solitary wave with $p = 3,\ c = 0.3, h = 0.1,\ \Delta t = 0.2,\ \varepsilon = 3,\ \mu = 1,\ x \in [0, 80]$ at $t = 20$.

Method	I_1	I_2	I_3	L_2	L_∞
Our Method	2.8043743	2.4639418	0.9855971	0.00454007	0.00341543
Cubic Galerkin[12]	2.8187398	2.4852249	1.0070200	0.01655637	0.01370453
Quintic Collocation First Scheme[36]	2.8043570	2.4639086	0.9855602	0.00801470	0.00538237
Quintic Collocation Second Scheme[36]	2.8042943	2.4637495	0.9854011	0.00708553	0.00480470
Petrov-Galerkin[37]	2.80436	2.46389	0.98556	0.00484271	0.00370926

For the second set, we select the parameters $p = 3,\ c = 0.3,\ h = 0.1,\ \Delta t = 0.2,\ \varepsilon = 3,\ \mu = 1,\ x_0 = 30$ with interval [0, 80] to coincide with that of previous papers[12,36,37]. Thus the solitary wave has amplitude 1.0 and the computations are carried out for times up to $t = 20$. The error norms L_2, L_∞ and conservation quantities I_1, I_2 and I_3 are computed, which are given in the Table 3). According to Table 3 the error norms L_2 and L_∞ remain less than 5.54007×10^{-3} and 3.41543×10^{-3}, the invariants I_1, I_2 and I_3 change from their initial values by less than 1.63×10^{-5}, 4.09×10^{-5} and 3.53×10^{-5}, respectively, throughout the simulation. Also, our invariants are almost constant as time increases. Therefore we can say our method is satisfactorily conservative. In Table 4 the performance of the our new method is compared with other methods [12,36,37] at $t = 20$. It is observed that errors of the method [12,36,37] are considerably larger than those obtained with the present scheme. Fig. 3 shows the solutions at $t = 0, 10, 20$. It is clear from the figure that the single soliton moved to the right with the preserved amplitude and shape. The amplitude is 1.00000 at $t = 0$ and located at $x = 30$, while it is 0.999522 at $t = 20$ and located at $x = 36$. Therefore the absolute difference in amplitudes over the time interval [0,20] are found as 4.78×10^{-4}. The aberration of error at discrete times are designed in Fig. 4. The error deviation varies from -3×10^{-3} to 4×10^{-3}.

Finally, we have taken the parameters $p = 4,\ c = 0.2,\ h = 0.1,\ \Delta t = 0.2,\ \varepsilon = 3,\ \mu = 1,\ x_0 = 30$ over the region [0,80] to compare with those of earlier papers [12,36,37]. Thereby, solitary wave has amplitude 1.0 and the simulations are executed to time $t = 20$ to invent the error norms L_2 and L_∞ and the numerical invariants I_1, I_2 and I_3. For these values of the parameters, the conservation properties and the L_2-error as well as the L_∞-error norms have been given in Table 5 for various values of the time level t. It can be noted from Table 5, the error norms L_2 and L_∞ remain less than 2.01343×10^{-3} and 1.41097×10^{-3}, the invariants I_1, I_2 and I_3 change from their initial values by less than 4.01×10^{-5},9.26×10^{-5} and 8.28×10^{-5}, respectively, throughout the simulation. Also, our invariants are almost constant as time increases and the changes of the invariants agree with their exact values. Therefore we can say our method is sensibly conservative. The comparison between the results obtained by the present method with those in the other studies [12,36,37] is also documented in Table 6. It is noticeably seen from the table that errors of the present method are radically less than those obtained with the earlier schemes [12,36,37]. For visual representation, the simulations of single soliton for values $p = 4, c = 0.2, h = 0.1, \Delta t = 0.2$ at times $t = 0, 10$ and 20 are illustrated in Fig. 5. It is understood from this gure that the numerical

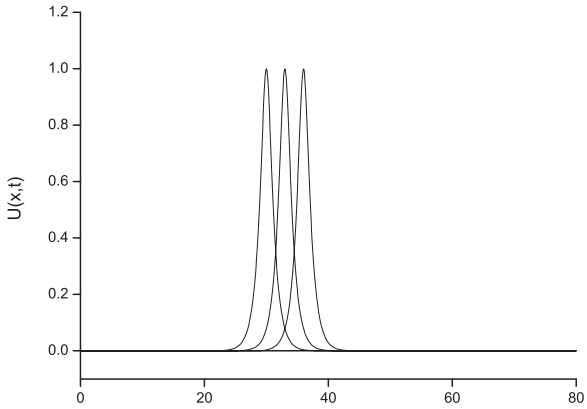

Fig. 3. Motion of single solitary wave for $p = 3,\ c = 0.3,\ h = 0.1,\ \Delta t = 0.2,\ \varepsilon = 3,\ \mu = 1,\ x \in [0, 80]$ at $t = 0, 10, 20$.

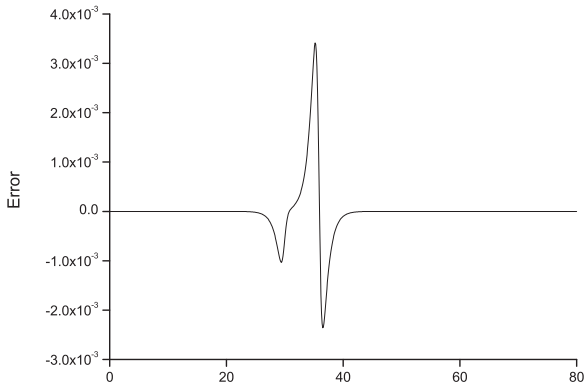

Fig. 4. Error graph for $p = 3,\ c = 0.3,\ h = 0.1,\ \Delta t = 0.2,\ \varepsilon = 3,\ \mu = 1,\ x \in [0, 80]$ at $t = 20$.

Table 5
Invariants and errors for single solitary wave with $p = 4,\ c = 0.2, h = 0.1,\ \Delta t = 0.2,\ \varepsilon = 3,\ \mu = 1,\ x \in [0, 80]$.

Time	I_1	I_2	I_3	L_2	L_∞
0	2.6220516	2.3561722	0.7853952	0.000000	0.000000
5	2.6220845	2.3562523	0.7854668	0.00126413	0.00143888
10	2.6220915	2.3562646	0.7854778	0.00181723	0.00151277
15	2.6220917	2.3562648	0.7854781	0.00197790	0.00145913
20	2.6220917	2.3562648	0.7854780	0.00201343	0.00141097

Table 6
Comparisons of results for single solitary wave with $p = 4,\ c = 0.2, h = 0.1,\ \Delta t = 0.2,\ \varepsilon = 3,\ \mu = 1,\ x \in [0, 100]$ at $t = 20$.

Method	I_1	I_2	I_3	L_2	L_∞
Our Method	2.6220917	2.3562648	0.7854780	0.00201343	0.00141097
Cubic Galerkin [12]	2.6327833	2.3730032	0.8023383	0.00890617	0.00821991
Quintic Collocation First Scheme [36]	2.6220508	2.3561901	0.7853939	0.00421697	0.00297952
Quintic Collocation First Scheme [36]	2.6219284	2.3559327	0.7851364	0.00339086	0.00247031
Petrov-Galerkin [37]	2.62206	2.35615	0.78534	0.00230499	0.00188285

scheme performs the motion of propagation of a single solitary wave, which moves to the right at nearly unchanged speed and conserves its amplitude and shape with increasing time. The amplitude is 1.00000 at $t = 0$ and located at $x = 30$, while it is 0.999478 at $t = 20$ and located at $x = 34$. The absolute difference in amplitudes at times $t = 0$ and $t = 10$ is 5.22×10^{-4} so that there is a little change between amplitudes. Error distributions at time $t = 20$ are shown graphically in Fig. 6. As it is seen, the maximum errors are between -1.5×10^{-3} to 1.5×10^{-3} and occur around the central position of the solitary wave.

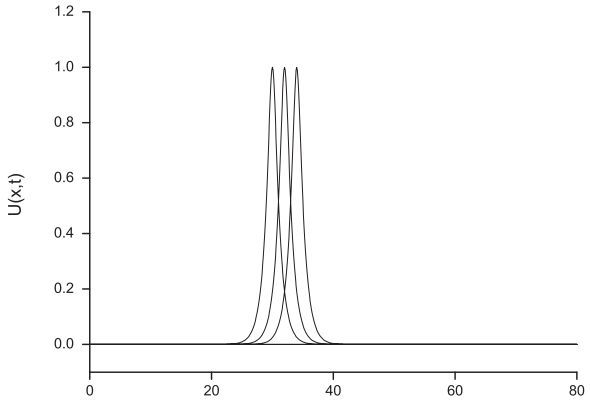

Fig. 5. Motion of single solitary wave for $p = 4, c = 0.2, h = 0.1, \Delta t = 0.2,\ \varepsilon = 3,\ \mu = 1, x \in [0, 80]$ at $t = 0, 10, 20$.

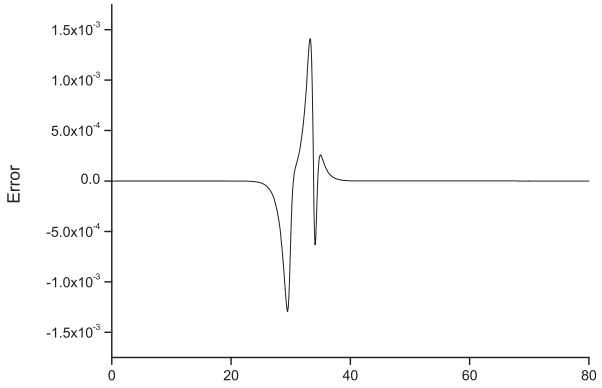

Fig. 6. Error graph for $p = 4,\ c = 0.2,\ h = 0.1,\ \Delta t = 0.2,\ \varepsilon = 3,\ \mu = 1$ at $t = 20$.

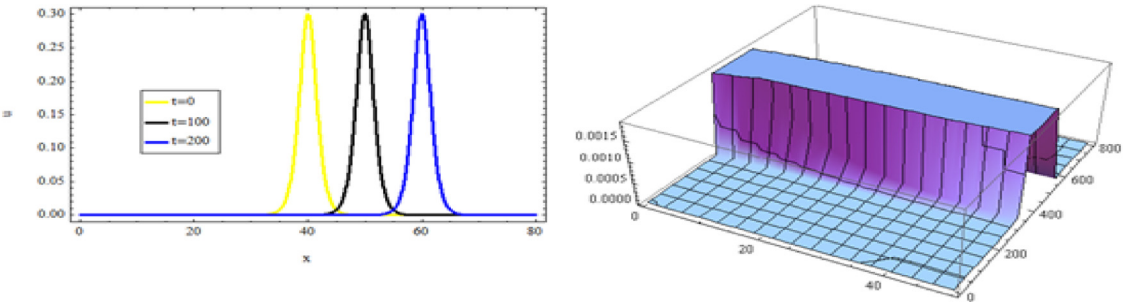

Fig. 7. Graph of case (5) for the EW equation.

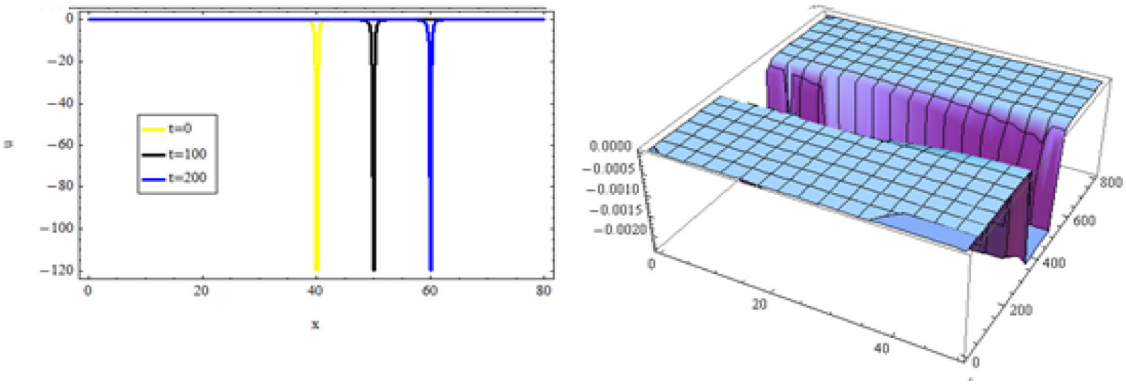

Fig. 8. Graph of case (6) for the EW equation.

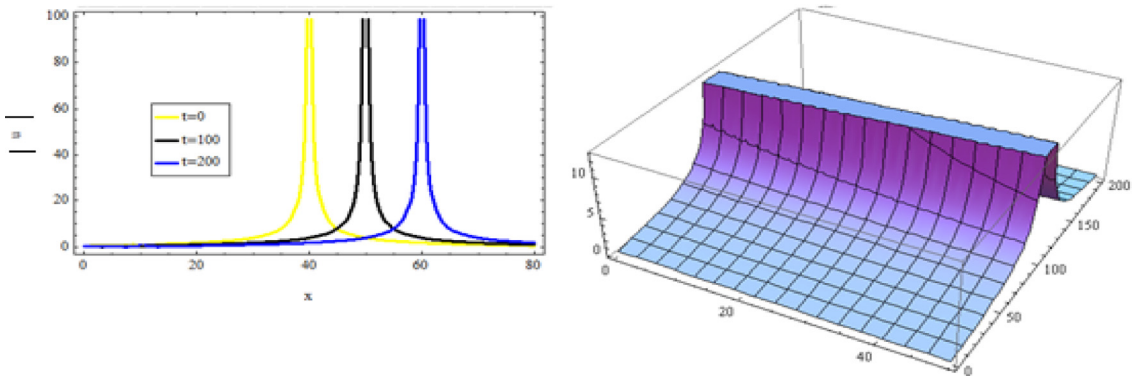

Fig. 9. Graph of case (2) for the MEW equation.

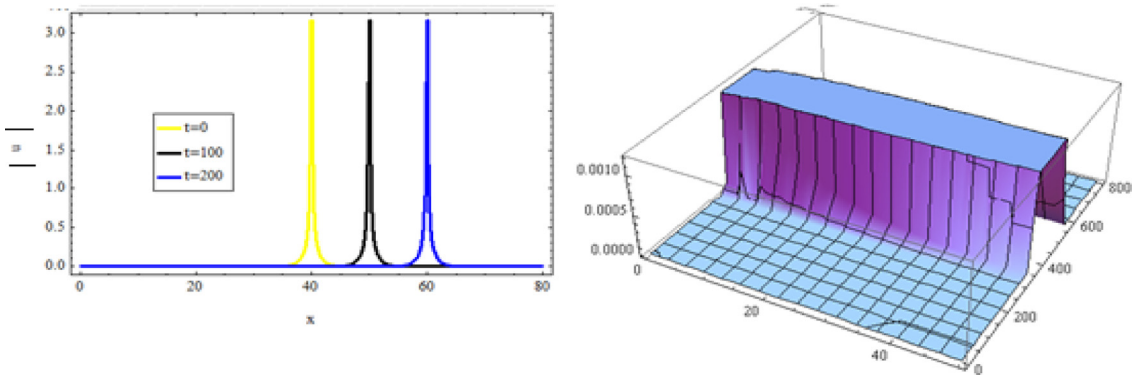

Fig. 10. Graph of case (3) for the MEW equation.

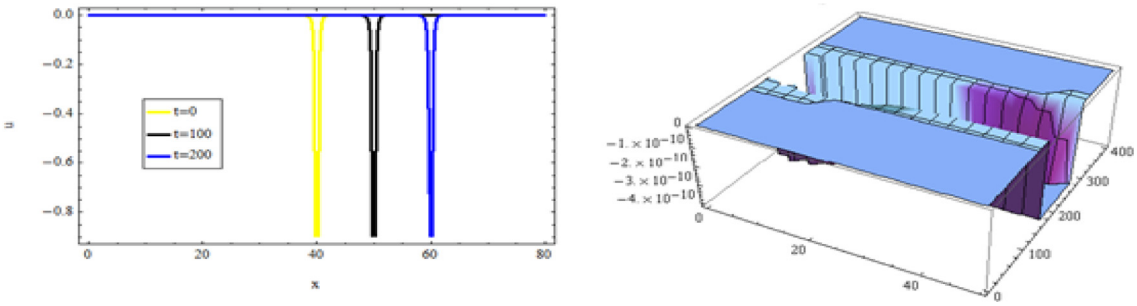

Fig. 11. Graph of case (2) for the GEW equation.

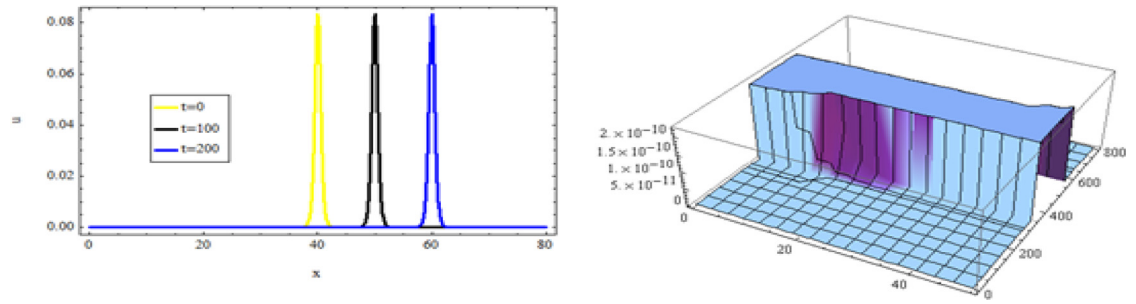

Fig. 12. Graph of case (3) for the GEW equation.

5. Description of the modified extended tanh function method with the Riccati equation

In this section, we use the modified extended tanh function method with the Riccati equation to find the exact solutions of the GEW equation. To illustrate the basic ideas of the method, consider the following nonlinear PDE with only two independent variables;

$$F(u, u_t, u_x, u_{tt}, u_{xt}, u_{xx}\ldots) = 0. \tag{24}$$

Applying the transformation

$$u(x,t) = f(\xi), \quad \xi = kx - ct - x_0, \tag{25}$$

where k and c are nonzero constants and x_0 is arbitrary constant, converts Eq. (24) into an integer order nonlinear ordinary differential equations as follows

$$H(f, \quad f', f'', f''', \ldots) = 0, \tag{26}$$

where the derivatives are with respect to ξ. It is assumed that the solutions of Eq. (26) are presented as a finite series, say

$$f(\xi) = a_0 + \sum_{n=1}^{N} \left(a_n \phi^n(\xi) + b_n \phi^{-n}(\xi)\right), \tag{27}$$

where a_n, b_n, $n = 1, 2, \ldots, N$ are constants can be computed, and $\phi^n(\xi)$ satisfies the Riccati equation

$$\phi' = d + \phi^2, \tag{28}$$

where d is a constant, Eq. (28) admits several types of solutions:

If $d < 0$ then

$$\phi = -\sqrt{-d}\tanh\left(\sqrt{-d}\xi\right) \quad or \quad \phi = -\sqrt{-d}\ \coth\left(\sqrt{-d}\xi\right).$$

If $d > 0$ then

$$\phi = \sqrt{d}\tan(\sqrt{d}\xi) \quad or \quad \phi = -\sqrt{d}\cot\left(\sqrt{d}\xi\right).$$

If $d = 0$ then

$$\phi = -\frac{1}{\xi}.$$

It should be mentioned that the value of N is usually determined by balancing the linear and nonlinear terms of highest orders in (26). Substituting Eq. (27) and its necessary derivatives, for example

$$f' = \sum_{n=1}^{N} \left(a_n n \ \phi^{n-1}\left(b + \phi^2\right) - \ b_n n \ \phi^{-n-1}\left(b + \phi^2\right)\right),$$

$$f'' = \sum_{n=1}^{N} \begin{pmatrix} a_n n(n-1)\phi^{n-2}\left(b + \phi^2\right)^{\ 2} + 2\ n a_n \phi^n\left(b + \phi^2\right) \\ + b_n n(n+1)\phi^{-n-2}\left(b + \phi^2\right)^{\ 2} - 2 b_n n \phi^{-n}\left(b + \phi^2\right) \end{pmatrix},$$

into (26) gives

$$P(\phi(\xi)) = 0, \tag{29}$$

where $P(\phi(\xi))$ is a polynomial in $\phi(\xi)$. By equating the coefficient of each power of $\phi(\xi)$ in (29) to zero, a system of algebraic equations will be obtained whose solution yields the exact solutions of (26).

6. Exact solutions of the GEW equation

Applying the wave transformation (25), we can reduce (4) to the nonlinear ordinary differential equation as the following:

$$-cf' + \varepsilon k f^p f' + \mu c k^2 f''' = 0. \tag{30}$$

Integrating (30) once with respect to ξ, yields

$$-cf + \varepsilon k \frac{1}{p+1}\ f^{p+1} + \mu c k^2 f'' = 0, \tag{31}$$

where the integrating constant is considered to be zero. Now we study these cases.

6.1. The exact solution of EW (at (p=1) in GEW) equation

If we put $p = 1$ into Eq. (31) we obtain:

$$-cf + \varepsilon k\ \frac{1}{2}\ f^2 + \mu c k^2 f'' = 0. \tag{32}$$

The value of N is usually determined by balancing $f''$and f^2in (32) results $N + 2 = 2N$ and so $N = 2$. This offers a truncated series as the following form:

$$f(\xi) = a_0 + a_1\phi(\xi) + b_1\phi^{-1}(\xi) + a_2\phi^2(\xi) + b_2\phi^{-2}(\xi). \tag{33}$$

By substituting (33) and its derivatives into (32) and equating the coefficient of each power of $\phi(\xi)$ to zero. We derive a system of algebraic equations as follows:

$$-ca_0 + \frac{1}{2}k\varepsilon a_0^2 + 2d^2ck^2\mu a_2 + k\varepsilon\ a_1b_1 + 2ck^2\mu b_2 + k\varepsilon\ a_2b_2 = 0,$$

$$6d^2ck^2\mu b_2 + \frac{k\varepsilon\ b_2^2}{2} = 0,$$

$$2d^2ck^2\mu b_1 + k\varepsilon b_1b_2 = 0,$$

$$\frac{k\varepsilon\ b_1^2}{2} - cb_2 + 8dck^2\mu b_2 + k\varepsilon\ a_0b_2 = 0,$$

$$-cb_1 + 2dck^2\mu b_1 + k\varepsilon a_0b_1 + k\varepsilon a_1b_2 = 0,$$

$$-ca_1 + 2dck^2\mu a_1 + k\varepsilon\ a_0a_1 + k\varepsilon\ a_2b_1 = 0,$$

$$\frac{1}{2}k\varepsilon\ a_1^2 - ca_2 + 8dck^2\mu a_2 + k\varepsilon a_0a_2 = 0,$$

$$2ck^2\mu a_1 + k\varepsilon a_1a_2 = 0,$$

$$6ck^2\mu a_2 + \frac{1}{2}\varepsilon a_2^2 = 0.$$

Solving the above system, yields;

Case 1.

$$a_0 = -\frac{c}{k\ \varepsilon},\ b_2 = 0,\ b_1 = 0,\ a_1 = 0,\ a_2 = -\frac{12ck\mu}{\varepsilon},\quad d = \frac{1}{4k^2\mu}.$$

Substituting into (33) and using (25) therefore, the solution of EW equation is formed as:

$$u_1(x,t) = -\frac{c}{k\ \varepsilon} - \frac{12ck\mu}{\varepsilon}\sqrt{d}\ tan\left(\sqrt{d}\xi\right),$$

$$u_2(x,t) = -\frac{c}{k\varepsilon} + \frac{12ck\mu}{\varepsilon}\sqrt{d}\ cot\left(\sqrt{d}\xi\right),$$

where $\xi = k\ \ x - c\ \ t - x_0$.

Case 2.

$$a_0 = -\frac{c}{k\varepsilon},\ b_2 = -\frac{3c}{4k^3\varepsilon\ \mu},\ a_2 = 0,\ b_1 = 0,\ a_1 = 0,\quad d = \frac{1}{4k^2\mu}.$$

Substituting into (33) and using (25) so, the solution of EW equation is formed as:

$$u_3(x,t) = -\frac{c}{k\ \varepsilon} - \frac{3c}{4k^3\varepsilon\mu d}\ cot^2\left(\sqrt{d}\xi\right),$$

$$u_4(x,t) = -\frac{c}{k\varepsilon} - \frac{3c}{4k^3\varepsilon\mu d}\ tan^2\left(\sqrt{d}\xi\right),$$

where $\xi = k\ \ x - c\ \ t - x_0$.

Case 3.

$$a_0 = \frac{c}{2k\varepsilon},\ b_2 = -\frac{3c}{64k^3\varepsilon\mu},\ b_1 = 0,\ a_1 = 0,\ a_2 = -\frac{12ck\mu}{\varepsilon},\quad d = \frac{1}{16k^2\mu}.$$

Substituting into (33) and using (25) hence, the solution of EW equation is formed as:

$$u_5(x,t) = \frac{c}{2k\varepsilon} - \frac{12ck\mu d}{\varepsilon}tan^2\left(\sqrt{d}\xi\right) - \frac{3c}{64k^3\varepsilon\mu d}\ cot^2\left(\sqrt{d}\xi\right),$$

$$u_6(x,t) = \frac{c}{2k\varepsilon} - \frac{12ck\mu d}{\varepsilon}cot^2\left(\sqrt{d}\xi\right) - \frac{3c}{64k^3\varepsilon\mu d}tan^2\left(\sqrt{d}\xi\right),$$

where $\xi = k\ \ x - c\ \ t - x_0$.

Case 4.

$$a_0 = \frac{3c}{2k\varepsilon}, b_2 = -\frac{3c}{64k^3\varepsilon\mu},\ a_1 = 0,\ a_2 = -\frac{12ck\mu}{\varepsilon},\quad d = -\frac{1}{16k^2\mu}.$$

Substituting into (33) and using (25) thereby, the solution of EW equation is formed as:

$$u_7(x,t) = \frac{3c}{2k\varepsilon} + \frac{12ck\mu d}{\varepsilon}\tan h^2\left(\sqrt{-d}\xi\right) + \frac{3c}{64k^3\varepsilon\mu d}\ \cot h^2\left(\sqrt{-d}\xi\right),$$

$$u_8(x,t) = \frac{3c}{2k\varepsilon} + \frac{12ck\mu d}{\varepsilon}\cot h^2\left(\sqrt{-d}\xi\right) + \frac{3c}{64k^3\varepsilon\mu d}\ \tan h^2\left(\sqrt{-d}\xi\right),$$

where $\xi = k\ \ x - c\ \ t - x_0$.

Case 5.

$$a_0 = \frac{3c}{k\varepsilon},\ b_2 = 0,\ b_1 = 0,\ a_1 = 0,\ a_2 = -\frac{12ck\mu}{\varepsilon},\quad d = -\frac{1}{4k^2\mu}.$$

Substituting into (33) and using (25) then, the solution of EW equation is formed as:

$$u_9(x,t) = \frac{3c}{k\varepsilon} + \frac{12ck\mu d}{\varepsilon}tanh^2\left(\sqrt{-d}\xi\right),$$

$$u_{10}(x,t) = \frac{3c}{k\varepsilon} + \frac{12ck\mu d}{\varepsilon}\cot h^2\left(\sqrt{-d}\xi\right),$$

where $\xi = k\ \ x - c\ \ t - x_0$.

Case 6.

$$a_0 = \frac{3c}{k\varepsilon},\ b_2 = -\frac{3c}{4k^3\varepsilon\mu},\ a_2 = 0,\ b_1 = 0,\ a_1 = 0,\ \ d = -\frac{1}{4k^2\mu}.$$

Substituting into (33) and using (25) consequently, the solution of EW equation is formed as:

$$u_{11}(x,t) = \frac{3c}{k\varepsilon} + \frac{3c}{4k^3\varepsilon\mu d}\ coth^2\left(\sqrt{-d}\xi\right),$$

$$u_{12}(x,t) = \frac{3c}{k\varepsilon} + \frac{3c}{4k^3\varepsilon\mu d}\ \tan h^2\left(\sqrt{-d}\xi\right),$$

where $\xi = k\ \ x - c\ \ t - x_0$.

6.2. The exact solution of MEW (at (p=2) in GEW) equation

If we put $p = 2$ into Eq. (31) we get:

$$-cf + \frac{1}{3}\varepsilon k f^3 + \mu c k^2 f'' = 0. \tag{34}$$

The value of N is usually determined by balancing $f''$and f^3 in (34) results $N + 2 = 3N$ and so $N = 1$. This offers a truncated series as the following form:

$$f(\xi) = a_0 + a_1\phi(\xi)\ \ + b_1\phi^{-1}(\xi)\ . \tag{35}$$

By substituting (35) and its derivatives into (34) and equating the coefficient of each power of $\phi(\xi)$ to zero. We derive a system of algebraic equations as follows:

$$-ca_0 + \frac{1}{3}k\varepsilon\ a_0^3 + 2k\varepsilon\ a_0a_1b_1 = 0,$$

$$2d^2ck^2\mu b_1 + \frac{k\varepsilon\ b_1^3}{3} = 0,$$

$$k\varepsilon a_0 b_1^2 = 0,$$

$$-cb_1 + 2dck^2\mu b_1 + k\varepsilon a_0^2 b_1 + k\varepsilon a_1 b_1^2 = 0,$$

$$-ca_1 + 2dck^2\mu a_1 + k\varepsilon a_0^2 a_1 + k\varepsilon a_1^2 b_1 = 0,$$

$$k\varepsilon a_0 a_1^2 = 0,$$

$$2ck^2\mu a_1 + \frac{1}{3}k\varepsilon a_1^3 = 0,$$

Solving the above system, yields;

Case 1.

$$d = \frac{1}{2k^2\mu},\ b_1 = 0,\ a_0 = 0,\ a_1 = \mp\frac{i\sqrt{6}\sqrt{c}\sqrt{k}\sqrt{\mu}}{\sqrt{\varepsilon}}.$$

Substituting into (35) and using (25) therefore, the solution of MEW equation is formed as:

$$u_1(x,t) = \mp\frac{i\sqrt{6}\sqrt{c}\sqrt{k}\sqrt{\mu}}{\sqrt{\varepsilon}}\sqrt{d}\ tan\left(\sqrt{d}\xi\right),$$

$$u_2(x,t) = \pm\frac{i\sqrt{6}\sqrt{c}\sqrt{k}\sqrt{\mu}}{\sqrt{\varepsilon}}\sqrt{d}\ cot\left(\sqrt{d}\xi\right),$$

where $\xi = k\ \ x - c\ \ t - x_0$.

Case 2.

$$a_0 = 0,\ a_1 = \mp\frac{i\sqrt{6}\sqrt{c}\sqrt{k}\sqrt{\mu}}{\sqrt{\varepsilon}},\ b_1 = \pm\frac{i\sqrt{\frac{3}{2}}\sqrt{c}}{4k^{3/2}\sqrt{\varepsilon}\sqrt{\mu}},\quad d = \frac{1}{8k^2\mu}.$$

Substituting into (35) and using (25) thus, the solution of MEW equation is formed as:

$$u_3(x,t) = \mp\frac{i\sqrt{6}\sqrt{c}\sqrt{k}\sqrt{\mu}}{\sqrt{\varepsilon}}\sqrt{d}\ tan\left(\sqrt{d}\xi\right) \pm \frac{i\sqrt{\frac{3}{2}}\sqrt{c}}{4k^{3/2}\sqrt{\varepsilon}\sqrt{\mu}\sqrt{d}}cot\left(\sqrt{d}\xi\right),$$

$$u_4(x,t) = \mp\frac{i\sqrt{6}\sqrt{c}\sqrt{k}\sqrt{\mu}}{\sqrt{\varepsilon}}\sqrt{d}\ \cot\left(\sqrt{d}\xi\right) \pm \frac{i\sqrt{\frac{3}{2}}\sqrt{c}}{4k^{3/2}\sqrt{\varepsilon}\sqrt{\mu}\sqrt{d}}\tan\left(\sqrt{d}\xi\right),$$

where $\xi = k\ \ x - c\ \ t - x_0$.

Case 3.

$$a_0 = 0,\ a_1 = \mp\frac{i\sqrt{6}\sqrt{c}\sqrt{k}\sqrt{\mu}}{\sqrt{\varepsilon}},\ b_1 = \pm\frac{i\sqrt{\frac{3}{2}}\sqrt{c}}{2k^{3/2}\sqrt{\varepsilon}\sqrt{\mu}},\quad d = -\frac{1}{4k^2\mu}.$$

Substituting into (35) and using (25) so, the solution of MEW equation is formed as:

$$u_5(x,t) = \pm\frac{i\sqrt{6}\sqrt{c}\sqrt{k}\sqrt{\mu}}{\sqrt{\varepsilon}}\sqrt{-d}\ tanh\left(\sqrt{-d}\xi\right) \mp \frac{i\sqrt{\frac{3}{2}}\sqrt{c}}{2k^{3/2}\sqrt{\varepsilon}\sqrt{\mu}\sqrt{-d}}\ \cot h\left(\sqrt{-d}\xi\right),$$

$$u_6(x,t) = \pm\frac{i\sqrt{6}\sqrt{c}\sqrt{k}\sqrt{\mu}}{\sqrt{\varepsilon}}\sqrt{-d}\ \cot h\left(\sqrt{-d}\xi\right) \mp \frac{i\sqrt{\frac{3}{2}}\sqrt{c}}{2k^{3/2}\sqrt{\varepsilon}\sqrt{\mu}\sqrt{-d}}\ \tan h\left(\sqrt{-d}\xi\right),$$

where $\xi = k\ \ x - c\ \ t - x_0$.

Case 4.

$$a_1 = 0,\ a_0 = 0,\ b_1 = \mp\frac{i\sqrt{\frac{3}{2}}\sqrt{c}}{k^{3/2}\sqrt{\varepsilon}\sqrt{\mu}},\quad d = \frac{1}{2k^2\imath}.$$

Substituting into (35) and using (25) hence, the solution of MEW equation is formed as:

$$u_7(x,t) = \mp\frac{i\sqrt{\frac{3}{2}}\sqrt{c}}{k^{3/2}\sqrt{\varepsilon}\sqrt{\mu}\sqrt{d}}\ cot\left(\sqrt{d}\xi\right),$$

$$u_8(x,t) = \pm\frac{i\sqrt{\frac{3}{2}}\sqrt{c}}{k^{3/2}\sqrt{\varepsilon}\sqrt{\mu}\sqrt{d}}\ tan\left(\sqrt{d}\xi\right),$$

where $\xi = k\ \ x - c\ \ t - x_0$.

6.3. The exact solution of GEW (at (p=3)) equation

If we put $p = 3$ into Eq. (31) we get:

$$-c\ f + \frac{1}{4}\varepsilon k f^4 + \mu c k^2 f'' = 0. \tag{36}$$

Balancing $f''$and f^4in (36) results $N + 2 = 4N$, and so $N = \frac{2}{3}$ but we know that N must be positive integer number, so we choose the transformation function $f(\xi) = g^{1/3}(\xi)$ and substituting into (36), we get

$$-cg^2 + \frac{1}{4}\varepsilon k g^3 + \mu k^2 c\left(\frac{1}{3}gg'' - \frac{2}{9}g'^2\right) = 0. \tag{37}$$

Now, we make balancing gg'' and g^4 in (37) results $N + N + 2 = 3N$, and so $N = 2$. This offers a truncated series as the following form

$$g(\xi) = a_0 + a_1\ \phi(\xi) + b_1\ \phi^{-1}(\xi) + a_2\ \phi^2(\xi) + b_2\ \phi^{-2}(\xi). \tag{38}$$

By substituting (38) and its derivatives into (37) and equating the coefficient of each power of $\phi(\xi)$ to zero. We derive a system of algebraic equations as follows:

$$-ca_0^2 + \frac{1}{4}k\varepsilon a_0^3 - \frac{2}{9}cd^2k^2\mu a_1^2 + \frac{2}{3}cd^2k^2\mu a_0a_2 - 2ca_1b_1 + \frac{20}{9}cdk^2\mu a_1b_1 + \frac{3}{2}k\varepsilon a_0a_1b_1 - \frac{2}{9}ck^2\mu b_1^2 + \frac{3}{4}k\varepsilon a_2b_1^2$$
$$+\frac{2}{3}ck^2\mu a_0b_2 + \frac{3}{4}k\varepsilon a_1^2b_2 - 2ca_2b_2 + \frac{80}{9}cdk^2\mu a_2b_2 + \frac{3}{2}k\varepsilon a_0a_2b_2 = 0,$$

$$\frac{10cd^2k^2\mu b_2^2}{9} + \frac{k\varepsilon b_2^3}{4} = 0,$$

$$\frac{16cd^2k^2\mu b_1b_2}{9} + \frac{3k\varepsilon b_1b_2^2}{4} = 0,$$

$$\frac{4cd^2k^2\mu b_1^2}{9} + 2cd^2k^2\mu a_0b_2 + \frac{3k\varepsilon b_1^2b_2}{4} - cb_2^2 + \frac{8cdk^2\mu b_2^2}{9} + \frac{3k\varepsilon a_0b_2^2}{4} = 0,$$

$$\frac{2cd^2k^2\mu a_0b_1}{3} + \frac{k\varepsilon b_1^3}{4} + \frac{26cd^2k^2\mu a_1b_2}{9} - 2cb_1b_2 + \frac{14cdk^2\mu b_1b_2}{9} + \frac{3k\varepsilon a_0b_1b_2}{2} + \frac{3k\varepsilon a_1b_2^2}{4} = 0,$$

$$\frac{10cd^2k^2\mu a_1b_1}{9} - cb_1^2 + \frac{2cdk^2\mu b_1^2}{9} + \frac{3k\varepsilon a_0b_1^2}{4} - 2ca_0b_2 + \frac{8cdk^2\mu a_0b_2}{3}$$
$$+\frac{3k\varepsilon a_0^2b_2}{4} + \frac{40cd^2k^2\mu a_2b_2}{9} + \frac{3k\varepsilon a_1b_1b_2}{2} - \frac{2ck^2\mu b_2^2}{9} + \frac{3k\varepsilon a_2b_2^2}{4} = 0,$$

$$-2ca_0b_1 + \frac{2cdk^2\mu a_0b_1}{3} + \frac{3k\varepsilon a_0^2b_1}{4} + \frac{20cd^2k^2\mu a_2b_1}{9} + \frac{3k\varepsilon a_1b_1^2}{4}$$
$$-2ca_1b_2 + \frac{46cdk^2\mu a_1b_2}{9} + \frac{3k\varepsilon a_0a_1b_2}{2} - \frac{2ck^2\mu b_1b_2}{9} + \frac{3k\varepsilon a_2b_1b_2}{2} = 0,$$

$$-2ca_0a_1 + \frac{2}{3}cdk^2\mu a_0a_1 + \frac{3}{4}k\varepsilon a_0^2a_1 - \frac{2}{9}cd^2k^2\mu a_1a_2 + \frac{3}{4}k\varepsilon a_1^2b_1 - 2ca_2b_1$$
$$+\frac{46}{9}cdk^2\mu a_2b_1 + \frac{3}{2}k\varepsilon a_0a_2b_1 + \frac{20}{9}ck^2\mu a_1b_2 + \frac{3}{2}k\varepsilon a_1a_2b_2 = 0,$$

$$-ca_1^2+\frac{2}{9}cdk^2\mu a_1^2+\frac{3}{4}k\varepsilon a_0a_1^2-2ca_0a_2+\frac{8}{3}cdk^2\mu a_0a_2+\frac{3}{4}k\varepsilon a_0^2a_2$$
$$-\frac{2}{9}cd^2k^2\mu a_2^2+\frac{10}{9}ck^2\mu a_1b_1+\frac{3}{2}k\varepsilon a_1a_2b_1+\frac{40}{9}ck^2\mu a_2b_2+\frac{3}{4}k\varepsilon a_2^2b_2=0,$$

$$\frac{2}{3}ck^2\mu a_0a_1+\frac{1}{4}k\varepsilon a_1^3-2ca_1a_2+\frac{14}{9}cdk^2\mu a_1a_2+\frac{3}{2}k\varepsilon a_0a_1a_2+\frac{26}{9}ck^2\mu a_2b_1+\frac{3}{4}k\varepsilon a_2^2b_1=0,$$

$$\frac{4}{9}ck^2\mu a_1^2+2ck^2\mu a_0a_2+\frac{3}{4}k\varepsilon a_1^2a_2-ca_2^2+\frac{8}{9}cdk^2\mu a_2^2+\frac{3}{4}k\varepsilon a_0a_2^2=0,$$

$$\frac{16}{9}ck^2\mu a_1a_2+\frac{3}{4}k\varepsilon a_1a_2^2=0,$$

$$\frac{10}{9}ck^2\mu a_2^2+\frac{1}{4}k\varepsilon a_2^3=0.$$

Solving the above system, yields;

Case 1.

$$a_0=\frac{5c}{k\varepsilon},\ b_2=-\frac{45c}{32k^3\varepsilon\mu},\ a_2=-\frac{40ck\mu}{9\varepsilon},\ b_1=0,\ a_1=0,\quad d=-\frac{9}{16k^2\mu}.$$

Substituting into (38), we get the solution of (37).

Since $f(\xi)=g^{1/3}(\xi)$ and using (25) therefore, the solution of GEW equation is formed as:

$$u_1(x,t)=\left(\frac{5c}{k\varepsilon}+\frac{40ck\mu d}{9\varepsilon}tanh^2\left(\sqrt{-d}\xi\right)+\frac{45c}{32k^3\varepsilon\mu d}\cot h^2\left(\sqrt{-d}\xi\right)\right)^{1/3},$$

$$u_2(x,t)=\left(\frac{5c}{k\varepsilon}+\frac{40ck\mu d}{9\varepsilon}\cot h^2\left(\sqrt{-d}\xi\right)+\frac{45c}{32k^3\varepsilon\mu d}\tan h^2\left(\sqrt{-d}\xi\right)\right)^{1/3},$$

where $\xi=k\ \ x-c\ \ t-x_0$.

Case 2.

$$a_0=\frac{10c}{k\varepsilon},\ b_2=0,\ a_2=-\frac{40ck\mu}{9\varepsilon},\ b_1=0,\ a_1=0,\quad d=-\frac{9}{4k^2\mu}.$$

Substituting into (38), we obtain the solution of (37).

Since $f(\xi)=g^{1/3}(\xi)$ and using (25) thus, the solution of GEW equation is formed as:

$$u_3(x,t)=\left(\frac{10c}{k\varepsilon}+\frac{40ck\mu d}{9\varepsilon}tanh^2\left(\sqrt{-d}\xi\right)\right)^{1/3},$$

$$u_4(x,t)=\left(\frac{10c}{k\varepsilon}+\frac{40ck\mu d}{9\varepsilon}\cot h^2\left(\sqrt{-d}\xi\right)\right)^{1/3},$$

where $\xi=k\ \ x-c\ \ t-x_0$.

Case 3.

$$a_0=\frac{10c}{k\varepsilon},\ b_2=-\frac{45c}{2k^3\varepsilon\mu},\quad a_2=0,\ b_1=0,\ a_1=0,\quad d=-\frac{9}{4k^2\mu}.$$

Substituting into (38), we get the solution of (37).

Since $f(\xi)=g^{1/3}(\xi)$ and using (25) then, the solution of GEW equation is formed as:

$$u_1(x,t)=\left(\frac{10c}{k\varepsilon}+\frac{45c}{2k^3\varepsilon\mu d}\ coth^2\left(\sqrt{-d}\xi\right)\right)^{1/3},$$

$$u_2(x,t)=\left(\frac{10c}{k\varepsilon}+\frac{45c}{2k^3\varepsilon\mu d}\ \tan h^2\left(\sqrt{-d}\xi\right)\right)^{1/3},$$

where $\xi=k\ \ x-c\ \ t-x_0$.

6.4. Some graphical illustrations

We depict in this section some graphical illustrations of the obtained solutions for the GEW equation. To reveal the clear picture of the obtained solutions, both the two and three dimensional plots for the solutions are given.

7. Conclusion

In this work, GEW equation is extensively examined by employing two reliable methods. The first method is the powerful Petrov-Galerkin finite element method that gives soliton solutions while the second method is the modified extended tanh function method with the Riccati differential equation and yields different trigonometric and hyperbolic function solutions, respectively. The modified extended tanh function method is used to find new exact traveling wave solutions of the equation. The method has an advantage of being direct and concise enormous variety of solutions are obtained with the aid of Mathematica software. We experimented our algorithm along with single solitary wave in which the exact solution is known. Stability analysis have been done and the linearized numerical scheme have been obtained unconditionally stable. The accuracy of the method is investigated both L_2 and L_∞ error norms and the invariant quantities I_1, I_2 and I_3. The obtained numerical results indicate that the error norms are satisfactorily small and the conservation laws are marginally constant in all computer program run. We can see that our numerical scheme for the equation is more accurate than the other earlier schemes found in the literature. Therefore, our numerical and exact techniques are suitable for getting numerical solutions of partial differential equations.

References

[1] W. Malfiet, Solitary wave solutions of nonlinear wave equations, Am. J. Phys. 60 (7) (1992) 650–654.
[2] A.M. Wazwaz, The tanh method: solitons and periodic solutions for the Dodd-Bullough-Mikhailov and the Tzitzeica-Dodd-Bullough equations, Chaos Solitons Fractals 25 (1) (2005) 55–63.
[3] A.M. Wazwaz, The extended tanh method for new soliton solutions for many forms of the fifth-order-KdV equation, Appl. Math. Comput. 184 (2) (2007) 1002–1014.
[4] A.M. Wazwaz, The extended tanh method: exact solutions of the sine-Gordon and sinh-Gordon equations, Appl. Math. Comput. 167 (2005) 1196–1210.
[5] E. Fan, Y.C. Hon, Generalized tanh method extended to special types of nonlinear equations, Z. Naturforsch 57a (2002) 692–700.
[6] N. Taghizadeh, M. Mirazadeh, The modified extended tanh-function method with Riccati equation for solving nonlinear partial differential equations, Math. Aeterna 2 (2) (2012) 145–153.
[7] S.A. El-Wakil, M.A. Abdou, New exact travelling wave solutions using modified extended tanh-function method, Chaos Solitons Fractals 31 (4) (2007) 840–852.
[8] D.H. Peregrine, Calculations of the development of an undular bore, J. Fluid Mech. 25 (1996) 321–330.
[9] D.H. Peregrine, Long waves on a beach, J. Fluid Mech. 27 (1967) 815–827.
[10] T.B. Benjamin, J.L. Bona, J.J. Mahony, Model equations for waves in nonlinear dispersive systems, Philos. Trans. R. Soc. Lond. 227 (1972) 47–78.
[11] P.J. Morrison, J.D. Meiss, J.R. Carey, Scattering of RLW solitary waves, Physica 11D (1981) 324–336.
[12] S.B.G. Karakoc, H. Zeybek, A cubic b-spline Galerkin approach for the numerical simulation of the GEW equation, Stat. Optim. Inf. Comput. 4 (2016) 30–41. March
[13] D. Kaya, A numerical simulation of solitary-wave solutions of the generalized regularized long wave equation, Appl. Math. Comput. 149 (2004) 833–841.
[14] D. Kaya, S.M. El-Sayed, An application of the decomposition method for the generalized KdV and RLW equations, Chaos Solitons Fractals 17 (2003) 869–877.
[15] L.R.T. Gardner, G.A. Gardner, T. Geyikli, The boundary forced MKdV equation, J. Comput. Phys. 11 (1994) 5–12.
[16] R.K. Dodd, J.C. Eilbeck, J.D. Gibbon, H.C. Morris, Solitons and Nonlinear Wave Equations, Academic Press, New York, 1982.
[17] J.C. Lewis, J.A. Tjon, Resonant production of solitons in the RLW equation, Phys. Lett. A 73 (1979) 275–279, doi:10.1016/0375-9601(79)90532-2.
[18] H. Panahipour, Numerical simulation of GEW equation using RBF collocation method 2012 (2012), doi:10.5899/2012/cna-00059. Article ID cna-00059.
[19] K.R. Raslan, Collocation method using cubic b-spline for the generalised equal width equation, Int. J. Simul. Process Model. 2 (2006) 37–44.
[20] L.R.T. Gardner, G.A. Gardner, Solitary waves of the equal width wave equation, J. Comput. Phys. 101 (1) (1991) 218–223.
[21] L.R.T. Gardner, G.A. Gardner, F.A. Ayoup, N.K. Amein, Simulations of the EW undular bore, Commun. Numer. Meth. En. 13 (7) (1997) 583–592.
[22] S.I. Zaki, A least-squares finite element scheme for the EW equation, Comput. Methods Appl. Mech. Eng. 189 (2) (2000) 587–594.
[23] A. Esen, A numerical solution of the equal width wave equation by a lumped Galerkin method, Appl. Math. Comput. 168 (1) (2005) 270–282.
[24] B. Saka, A finite element method for equal width equation, Appl. Math. Comput. 175 (1) (2006) 730–747.
[25] I. Dag, B. Saka, Acubic b-spline collocation method for the EW equation, Math. Comput. Appl. 9 (3) (2004) 381–392.
[26] S.B.G. Karakoç, T. Geyikli, Numerical solution of the modified equal width wave equation, Int. J. Differ. Equ. 2012 (2012) 1–15.
[27] T. Geyikli, S.B.G. Karakoç, Petrov-galerkin method with cubic b-splines for solving the MEW equation, Bull. Belg. Math. Soc. Simon Stevin 19 (2012) 215–227.
[28] T. Geyikli, S.B.G. Karakoç, Septic b-spline collocation method for the numerical solution of the modified equal width wave equation, Appl. Math. 2 (2011) 739–749.
[29] T. Geyikli, S.B.G. Karakoc, Subdomain finite element method with quartic b-splines for the modified equal width wave equation, Comput. Math. Math. Phys. 55 (3) (2015) 410–421.
[30] S.B.G. Karakoc, Numerical solutions of the modified equal width wave equation with finite elements method, PhD thesisInonu University, Malatya, Turkey,
[31] A. Esen, A lumped Galerkin method for the numerical solution of the modified equal-width wave equation using quadratic b-splines, Int. J. Comput. Math. 83 (5–6) (2006) 449–459.
[32] B. Saka, Algorithms for numerical solution of the modified equal width wave equation using collocation method, Math. Comput. Model. 45 (9–10) (2007) 1096–1117.
[33] S. Hamdi, W.H. Enright, W.E. Schiesser, J.J. Gottlieb, Exact solutions of the generalized equal width wave equation, in: Proceedings of the International Conference on Computational Science and Its Applications, in: LNCS, vol. 2668, Springer-Verlag, 2003, pp. 725–734.
[34] D.J. Evans, K.R. Raslan, Solitary waves for the generalized equal width (GEW) equation, Int. J. Comput. Math. 82 (4) (2005) 445–455.
[35] N. Taghizadeh, M. Mirzazadeh, M. Akbari, M. Rahimian, Exact solutions for generalized equal width equation, Math. Sci. Lett. 2 (2013) 99–106.
[36] H. Zeybek, S.B.G. Karakoc, Application of the collocation method with b-splines to the GEW equation, Electron. Trans. Numer. Anal. 46 (2017) 71–88.
[37] T. Roshan, A Petrov–Galerkin method for solving the generalized regularized equal width (GEW) equation, J. Comput. Appl. Math. 235 (2011) 1641–1652.
[38] P.M. Prenter, Splines and Variational Methods, John Wiley & Sons, New York, NY.USA, 1975.